Journal of Engineering Mathematics **39:** 189–206, 2001.

Matched asymptotic expansions and the numerical treatment of viscous-inviscid interaction

A.E.P. VELDMAN
Institute of Mathematics and Computing Science, University of Groningen, P.O. Box 800, 9700 AV Groningen, The Netherlands (e-mail: veldman@math.rug.nl)

Received 14 January 2000; accepted in revised form 15 August 2000

Abstract. The paper presents a personal view on the history of viscous-inviscid interaction methods, a history closely related to the evolution of the method of matched asymptotic expansions. The main challenge in solving Prandtl's boundary-layer equations has been to overcome the singularity at a point of steady flow separation. Stewartson's triple-deck theory has inspired a solution to this challenge, and thereby it paved the way for industrial use of viscous-inviscid interaction methods.

Key words: boundary-layer separation, viscous-inviscid interaction, matched asymptotic expansions, numerical simulation, transonic airfoils

1. Prandtl's boundary layer

The history of the development of viscous-inviscid interaction methods started in Heidelberg at 11:30 a.m. on August 12, 1904, when Ludwig Prandtl presented the 'boundary layer' before an audience of mathematicians attending the Third International Mathematical Congress [1]. For decades, scientists had been confused by d'Alembert's Paradox ('discovered' in 1752), stating that "there is no drag on a finite body at rest in an infinite, incompressible, inviscid flow otherwise in uniform motion" [2]. Prandtl described how the hardly visible boundary layer near the surface of the body, through the influence of viscosity, can resolve this paradox.

Prandtl's Heidelberg lecture is considered a landmark in the development of a branch of mathematics nowadays called 'matched asymptotic expansions', although various roots of the boundary-layer idea can be found already in the nineteenth century [3]. The method of matched asymptotic expansions treats differential equations where a small parameter multiplies the highest derivative, *i.e.* setting the small parameter at zero implies dropping one (or more) boundary conditions. As a consequence a series development in the small parameter is no longer valid uniformly throughout the domain. Next to the boundary where in the small-parameter limit boundary conditions have to be dropped, a thin layer has to be added where a different series development is required. Prandtl named this thin layer *Grenzschicht* (English translation: boundary layer), a name that has been used ever since for similar thin layers in other applications.

In aerodynamic applications (Figure 1), the boundary layer is driven by the inviscid pressure distribution p_e and its (through Bernoulli's law) related streamwise velocity u_e. In the boundary layer the streamwise velocity component is reduced to zero in order to comply with the no-slip condition at the surface. The lateral coordinate y, together with its corresponding velocity component v, scales with the inverse square root of the Reynolds number Re (defined

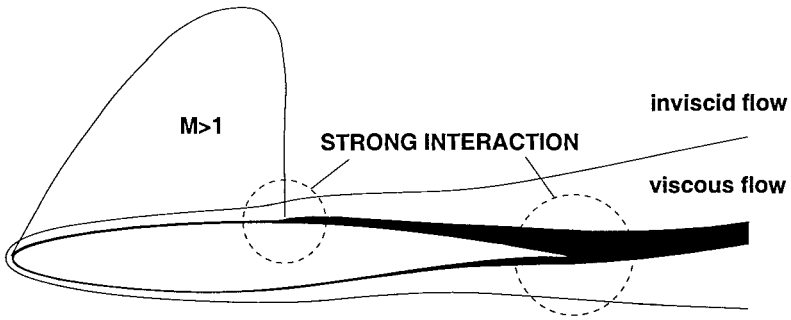

Figure 1. Subdivision of the flow field around an airfoil in an inviscid-flow region and a viscous shear layer (exaggerated in thickness).

in the usual way[1]). The flow equations can be simplified by neglecting the viscous streamwise derivatives, whereas the lateral momentum equation states the pressure to be constant through the boundary layer. Prandtl's *Grenzschichtgleichungen* emerge (in non-dimensional form):

$$\frac{\partial u}{\partial x} + \frac{\partial v}{\partial y} = 0, \quad u\frac{\partial u}{\partial x} + v\frac{\partial u}{\partial y} = u_e \frac{\mathrm{d}u_e}{\mathrm{d}x} + \frac{1}{\mathrm{Re}}\frac{\partial^2 u}{\partial y^2}, \tag{1}$$

with boundary conditions

$$u(x,0) = v(x,0) = 0; \quad u(x,y_e) = u_e,$$

where y_e denotes the outer edge of the boundary layer.

Effectively, the boundary layer changes (thickens and smoothes) the shape of the geometry. The resulting effective shape is called the displacement body $y = \delta^*$, which now becomes a streamline for the inviscid flow (*e.g.* Lighthill [4]).

The main advantage of the boundary-layer concept is that the elliptic character of the Navier–Stokes equations is changed into a much easier handled parabolic character. The latter was very relevant in an era when mainly analytical tools were available for solving differential equations. The stable direction of the boundary-layer equations (1) is governed by the sign of u. Hence this direction switches in reversed-flow regions, which has implications for the way they are solved, as we will see below.

2. Flow separation and solution breakdown

For situations with attached flow the boundary layer provides only a small perturbation to the inviscid-flow. However, it is found that as soon as the flow wants to separate from the body surface, the steady boundary-layer calculation breaks down with a solution that tends to become singular (*cf.* the conscientious discussion by Goldstein [5]). A number of possible causes can easily be imagined:

(i) The growth of the solution violates the assumption made in boundary-layer theory that streamwise derivatives should remain small. The remedy would be to include these streamwise derivatives in the equations of motion, but then the elliptic character of Navier–Stokes is retained with its corresponding much higher computational complexity.

[1]All variables have been made dimensionless with a characteristic length scale L and a characteristic velocity scale U. Re$= UL/\nu$, where ν is the kinematic viscosity.

(ii) The stable parabolic direction of the boundary-layer equations changes locally in reversed-flow regions, with negative streamwise velocity. As a consequence, in these regions the equations should be solved from downstream to upstream, hence one single downstream-marching computational sweep does not suffice any longer.

Now, one has to keep in mind that in the first half of the century there were hardly any appropriate tools to solve the flow equations. At that time it was impossible to check the above two possibilities, and the issue had to remain open.

In 1948 Goldstein presented an in-depth discussion on the breakdown of the boundary-layer equations at separation in which he added some more possible causes [5]. Since then, the singularity at separation bears his name. In particular, on page 50 of his paper, Goldstein formulates the following suggestion:

> "Another possibility is that a singularity will always occur except for certain special pressure variations in the neighbourhood of separation, and that, experimentally, whatever we may do, the pressure variations near separation will always be such that no singularity will occur. "

It took twenty more years before algorithms and computers were sufficiently developed to perform some numerical experiments in order to explore the options mentioned above. One of these experiments was described in 1966 by Catherall and Mangler [6], who tried to solve the steady boundary-layer equations with prescribed displacement thickness. Indeed, they succeeded to pass the point of flow separation, but ran into difficulties a bit further downstream. The reason hereof is clear, and in fact was already formulated by the authors [6, p. 178]: 'This is possibly to be expected, since the region of reversal flow should really be integrated in the negative ξ-direction with boundary conditions provided from downstream.' With current computer power, this problem is easily remedied by a downstream discretization of the convective terms and subsequent repeated sweeps through the boundary layer. Nevertheless, as Catherall and Mangler were not convinced of their success, they stopped further research into this subject. In fact, Catherall learned only some twenty years after publication about the large impact their paper had created, as he told me a few years ago.

3. The triple deck

In the late sixties, inspired by ideas put forward by Lighthill in 1953 [7], Stewartson (for steady subsonic and supersonic flow) [8, 9] and, independently, Messiter (subsonic) [10] and Neiland (supersonic) [11], developed asymptotic theories in the neighbourhood of singular points in the flow field, such as a trailing edge or a point of flow separation.

Therefore, let us consider a narrow region around such a singular point S, of extent

$$x - x_S = O(\mathrm{Re}^{-\alpha}), \quad 0 < \alpha < \tfrac{1}{2}, \quad \text{with a scaled coordinate } x_\alpha = (x - x_S)\mathrm{Re}^{\alpha},$$

where x-derivatives will be more important than assumed thus far. The restriction $\alpha < \frac{1}{2}$ implies that the width is larger than the boundary-layer thickness; hence x-derivatives remain less important than y-derivatives, which simplifies the analysis. Further it may be anticipated that in vertical direction close to the singular point something happens: say at a y-scale given by $\mathrm{Re}^{-\beta}$ with $\beta > \frac{1}{2}$ (which is smaller than the boundary-layer thickness).

Of course, the oncoming boundary-layer thickness $y = O(\mathrm{Re}^{-1/2})$ will play a role as well. Here the velocity profile immediately before the singular point can be written as ($\tilde{y} = \mathrm{Re}^{1/2} y$)

$$u(x_s,\ y) = \beta'(\tilde{y}) + O(\mathrm{Re}^{-1/2}), \quad \text{where for } \tilde{y} \downarrow 0 : B(\tilde{y} \sim \tfrac{1}{2} a \tilde{y}^2. \tag{2}$$

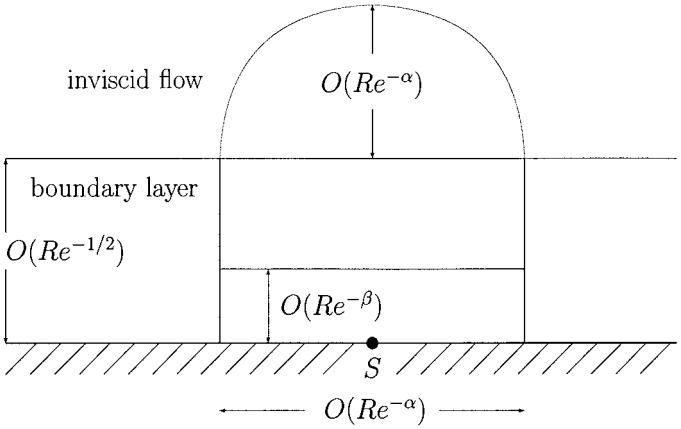

Figure 2. The triple deck describes the asymptotic flow structure near singular points.

The function $B'(\tilde{y})$ is known, *e.g.* it is a Blasius profile where $a = 0{\cdot}332$. Also the y-scale $y = O(\mathrm{Re}^{-\alpha})$ will play a role, since there x-derivatives are as large as y-derivatives.

This three-layered structure, called the triple deck, is sketched in Figure 2. What is left to find are the particular values for α and β, the modelling pertinent to the individual flow domains, and the flow of information between the separate decks. The latter point turns out to be of crucial importance for the design of numerical solution methods.

To obtain the required insight into the triple-deck behaviour it is unavoidable to go into some detail, therefore we will next give a short resume of the derivation of the (incompressible) triple deck.

3.1. THE LOWER DECK $y = O(\mathrm{Re}^{-\beta})$

In the lower deck the viscous terms balance with the convective terms. From (2) it follows that the oncoming velocity profile at small values of $\tilde{y}$ is given by $u \sim a\tilde{y}$. Hence for $y = O(\mathrm{Re}^{-\beta})$ the horizontal velocity is of magnitude $u = O(\mathrm{Re}^{1/2-\beta})$. An estimate of the convective and diffusive terms gives for $x = O(\mathrm{Re}^{-\alpha})$:

$$\text{convection: } u\frac{\partial u}{\partial x} = O(\mathrm{Re}^{1-2\beta+\alpha})\ ; \qquad \text{diffusion: } \frac{1}{\mathrm{Re}}\frac{\partial^2 u}{\partial y^2} = O(\mathrm{Re}^{\beta-1/2}).$$

Balancing these terms yields a relation between α and β

$$\beta = \frac{\alpha}{3} + \frac{1}{2}. \tag{3}$$

With this value of β the horizontal velocity scales like $u = O(\mathrm{Re}^{-\alpha/3})$, whereas the balancing pressure gradient corresponds with $p = O(\mathrm{Re}^{-2\alpha/3})$.

After substitution of these estimates in the Navier–Stokes equations it follows that the flow in the lower deck is still governed by Prandtl's boundary-layer equations, with a pressure that is again constant in the vertical direction: $p(x, y) = \mathrm{Re}^{-2\alpha/3}P(x_\alpha)$. High in the lower deck, for $y_\beta = \mathrm{Re}^{\beta}y \to \infty$, we have

$$u(x_\alpha, y_\beta) \sim \mathrm{Re}^{-\alpha/3}\{ay_\beta + aG(x_\alpha) + \cdots\}. \tag{4}$$

The function G is related to the displacement thickness, as will be clear in (6) below.

Next to the solid-wall conditions at $y_\beta = 0$, as a first boundary condition at infinity the coefficient of y_β (*i.e.* a) is given. Additionally, another boundary condition is required. In the classical interpretation this would be the prescription of the pressure, *i.e.* $P(x_\alpha)$, but in the spirit of Catherall and Mangler [6] this could also be a displacement effect, *i.e.* $G(x_\alpha)$.

It is stressed that in this way the lower-deck equations form one relation between P and G. A second relation can be found by matching with the other decks, as will be described next.

3.2. THE MIDDLE DECK $y = O(\mathrm{Re}^{-1/2})$

In order to concentrate on the essential properties of the triple deck, the derivation of the asymptotic expansions in the middle deck is only summarized (refer to the original papers by Stewartson [8] and Messiter [10], or to a later paper by Meyer [12]).

The middle deck is determined through matching with the oncoming flow (2) and the lower deck (3). It 'simply' shows a vertical shift of the oncoming velocity profile, caused by the displacement effect of the lower deck. The expansions in the middle deck are

$$u(x, y) \sim B'(\tilde{y}) + \mathrm{Re}^{-\alpha/3} B''(\tilde{y}) G(x_\alpha) + \cdots, \tag{5}$$

$$v(x, y) \sim -\mathrm{Re}^{2\alpha/3-1/2} B'(\tilde{y}) G'(x_\alpha) + \cdots. \tag{6}$$

Once again, the leading term in the pressure turns out to be constant in the y-direction: $p(x, y) \sim \mathrm{Re}^{-2\alpha/3} P(x_\alpha)$. This information is now passed on to the upper deck.

3.3. THE UPPER DECK $y = O(\mathrm{Re}^{-\alpha})$

In the upper deck the x- and y-dimensions are equal, whereas the viscous effects are not important. It is governed by inviscid flow where Laplace's equation and Bernoulli's law hold.

Since $B'(\tilde{y}) \to 1$ as $\tilde{y} \to \infty$, the vertical velocity (6) induces a vertical velocity $-\mathrm{Re}^{2\alpha/3-1/2} G'(x_\alpha)$ in the upper deck. According to Laplace's, a horizontal velocity perturbation $\tilde{u}$ of the same order is to be expected; in fact it is given by

$$\tilde{u}(x_\alpha, y_\alpha) = -\frac{1}{\pi} \mathrm{Re}^{2\alpha/3-1/2} \int_{-\infty}^{\infty} \frac{G'(\xi)(x - \xi)}{(x_\alpha - \xi)^2 + y_\alpha^2} \, \mathrm{d}\xi. \tag{7}$$

When in Bernoulli's law $p + (u^2 + v^2)/2 = C$ one substitutes $u = 1 + \tilde{u}$ and $v = \tilde{v}$, with $\tilde{u} \ll 1$ and $\tilde{v} \ll 1$, then to first approximation

$$p + \tilde{u} = C - \tfrac{1}{2}. \tag{8}$$

This implies that also the pressure expansion contains a term of order $\mathrm{Re}^{2\alpha/3-1/2}$, which hence is related to displacement effects.

Matching of middle and upper deck now yields two kinds of pressure terms in an expansion that reads

$$p(x, y) = \mathrm{Re}^{-2\alpha/3} p^{(p)}(x_\alpha, y_\alpha) + \mathrm{Re}^{2\alpha/3-1/2} p^{(\delta)}(x_\alpha, y_\alpha) + \cdots. \tag{9}$$

The term $p^{(p)}$ matches the pressure in the middle deck, so that it satisfies $p^{(p)}(x_\alpha, 0) = P(x_\alpha)$; the term $p^{(\delta)}$ arises due to displacement effects and through (8) is related to the horizontal velocity perturbation given by (7).

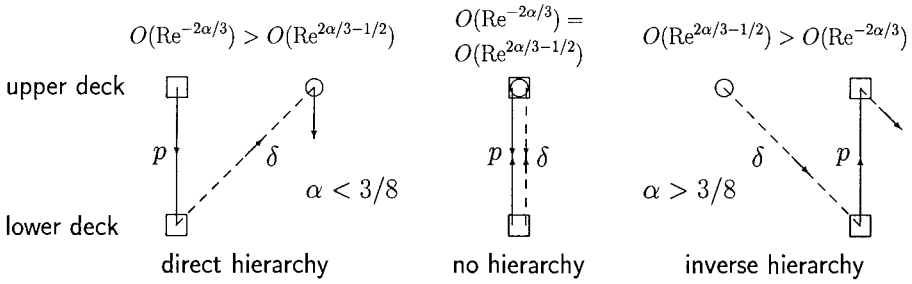

Figure 3. Hierarchy between pressure contributions in lower and upper deck at a streamwise lengthscale $x = O(\mathrm{Re}^{-\alpha})$.

3.4. Loss of hierarchy

Figure 3 shows the relative order of the two terms present in (9), and herewith it reveals the essential character of the triple deck as we will see.

When $\alpha < 3/8$ the term $p^{(p)}$ is the larger one in (9), and it determines, as usual, the pressure P in the boundary layer. The lower-deck equations then provide G after which the second term $p^{(\delta)}$ can be determined, which in turn provides a pressure correction in the boundary layer. The classical hierarchy between inviscid flow and boundary layer is recognized.

This situation changes for $\alpha = 3/8$ when both pressure terms in (9) are equally important, and this is what constitutes the essence of the triple deck. The pressure terms $p^{(p)}$ and $p^{(\delta)}$ have to be identical; thus by equating their values at $y_\alpha = 0$, from (7) and (8) a second relation between P and G is obtained:

$$P(x_\alpha) = \frac{1}{\pi} \int_{-\infty}^{\infty} \frac{G'(\xi)}{x_\alpha - \xi} \, \mathrm{d}\xi. \tag{10}$$

The triple-deck equations now consist of Prandtl's boundary-layer equations, with boundary condition (4) and a second relation between pressure and displacement given by a Cauchy–Hilbert integral (10).

Finally, for $\alpha > 3/8$ the displacement pressure $p^{(\delta)}$ is larger than $p^{(p)}$. Hence the hierarchy inverts, and the pressure is essentially determined in the lower deck.

Parallel to the above subsonic triple-deck, a supersonic version was developed by Stewartson and Williams [9]. Except for the description of the interaction, it is similar, to the inviscid flow. The *global* Cauchy-Hilbert integral (10) is replaced by a *local* Prandtl-Meyer relation

$$P(x_\alpha) = -G'(x_\alpha). \tag{11}$$

The triple deck has inspired a wealth of research on asymptotic descriptions; refer *e.g.* to the review papers by Stewartson [13] and Smith et al. [14–17] and the monograph by Sychev et al. [18].

3.5. Consequences for the numerical treatment

Because of its hyperbolic character the numerical treatment of the supersonic equations is relatively easy: in the absence of reversed flow a single marching sweep through the boundary layer suffices. A solution was presented already, together with their first formulation by

Stewartson and Williams [9], leaving the authors somewhat surprised that, even with reversed flow, their single marching sweep did not tend to become unstable.

The elliptic character of the subsonic triple-deck equations posed a larger challenge, however. It took half a decade before the first full (numerical) solutions were presented [19–21]. With hindsight, today the essence of the numerical obstinacy can 'easily' be understood. In the triple deck the boundary layer is no longer merely providing small corrections to the flow, but instead wants to have an equal say in determining the flow field. In aerodynamical terms, the hierarchy between boundary layer and inviscid flow changes from *weak* interaction into *strong* interaction. Lagerstrom [22, p. 209] in 1975 described the spirit of the triple deck as follows:

> "An important feature is that the pressure is self-induced, that is, the pressure due to displacement thickness is determined simultaneously with the revised boundary-layer solution. [...] this solution exhibits a definite loss of hierarchy."

This lack of hierarchy should also be visible in the numerical information exchange between boundary layer and inviscid flow, thus guiding their appropriate numerical iterative treatment; see Section 5.

Sixteen years earlier, Hayes and Probstein in their monograph on hypersonic flow [23, p. 365] came to a similar conclusion about the boundary-layer interaction near a point of flow separation:

> " ... in general it requires solving simultaneously the integrated momentum and energy equations and the inviscid flow relation describing the pressure along the curve $y = \delta^*(x)$. "

One should realise, of course, that here the inviscid flow is supersonic and the displacement effect of the boundary layer is described by the local Prandtl–Meyer fan (11). Nevertheless, the notion 'simultaneous' was already present!

Remark

The above interactive boundary-layer concept is restricted to mildly separated flows, *i.e.* flows where the thickness of the reversed-flow region is comparable to the boundary-layer thickness. For larger regions of reversed flow (marginal separation or, larger still, massive separation), the asymptotic structure has to be revised [24, 25]. At the same time, the flow in these larger separated-flow regions physically becomes unstable: an unsteady boundary-layer model has to be used, whose validity, in turn, terminates with a Van Dommelen-Shen singularity [26]. In a consistent way, numerical simulation methods based on the thin-boundary-layer concept tend to break down when the thickness of the separated-flow region becomes significant, *e.g.* [27], thus giving a warning that the selected flow modelling should be reconsidered. Readers might wish to consult Chapter 14 of the enlarged edition of Schlichting's 'Boundary-Layer Theory' [28] for a more detailed discussion of these asymptotic issues.

4. Non-asymptotic points of view

In the late seventies the quest for the cause of the singularity has also moved along non-asymptotic lines, which in retrospect can be related to the above. Several investigations into the boundary-layer relation between pressure and displacement thickness have been carried out, which all produced a similar outcome.

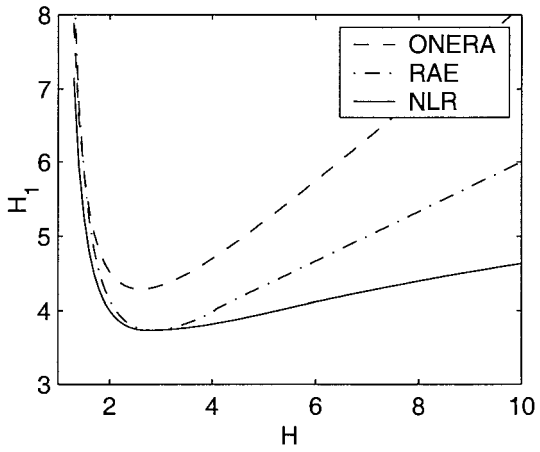

Figure 4. Some H-H_1 relationships as used at ONERA [29], RAE [30] and NLR [31] around 1980. The three relations agree on having a minimum somewhere near $H \approx 2.7$, corresponding with the onset of separation. For larger values of H the curves disagree, but experimental data to support these curves was rare at that time.

First, we will present the reflections of LeBalleur [29] at ONERA in France. He considered an integral formulation of the turbulent boundary-layer equations, consisting of Von Kármán's integral equation and Head's entrainment equation. In case u_e is prescribed, these differential equations are conveniently ordered as

$$\begin{aligned} \text{Von Kármán:}\quad & \frac{\mathrm{d}\theta}{\mathrm{d}x} && = \tfrac{1}{2}c_f - \frac{\theta}{u_e}(2+H)\frac{\mathrm{d}u_e}{\mathrm{d}x}, \\ \text{Entrainment:}\quad & H_1\frac{\mathrm{d}\theta}{\mathrm{d}x} + \theta\frac{\mathrm{d}H_1}{\mathrm{d}x} && = \frac{E}{u_e} - \frac{\theta H_1}{u_e}\frac{\mathrm{d}u_e}{\mathrm{d}x}. \end{aligned} \tag{12}$$

Here, θ is the momentum thickness, H the shape factor θ/δ^*, c_f the shear-stress coefficient, E Head's entrainment function and H_1 the entrainment shape factor (which is assumed to be a function of H only). The two differential equations are supplemented with three algebraic relations for determining H, E and c_f.

LeBalleur [29] demonstrated that the numerical problems at separation are caused by the algebraic relation between H and H_1. Since H_1 follows from the two differential equations (12), the algebraic relation should provide H. However, the graph of H_1 as a function of H shows a minimum at (or nearby) a point of flow separation. Figure 4 gives versions of this relation as used at ONERA [29], RAE [30] and NLR [31] around that time; supporting experimental data can be found in the review paper by Lock and Williams [32]. As a consequence, not for every value of H_1 is it possible to find a value for H! LeBalleur further showed that, when also u_e is considered an unknown, no difficulties arise (an extra equation has to be added that describes the coupling between inviscid flow and boundary layer).

As another example, a numerical experiment performed at the National Aerospace Laboratory (NLR) in Amsterdam will be described [33]. In this study the original boundary-layer equations (1), *i.e.* as a field method, were solved with a prescribed displacement thickness chosen such that flow separation occurred. Then at a fixed x-station δ^* was varied, keeping every other station fixed, and the variations of u_e and the shear-stress coefficient c_f were studied. It turned out that in this way u_e as a function of δ^* possessed a minimum that seemed

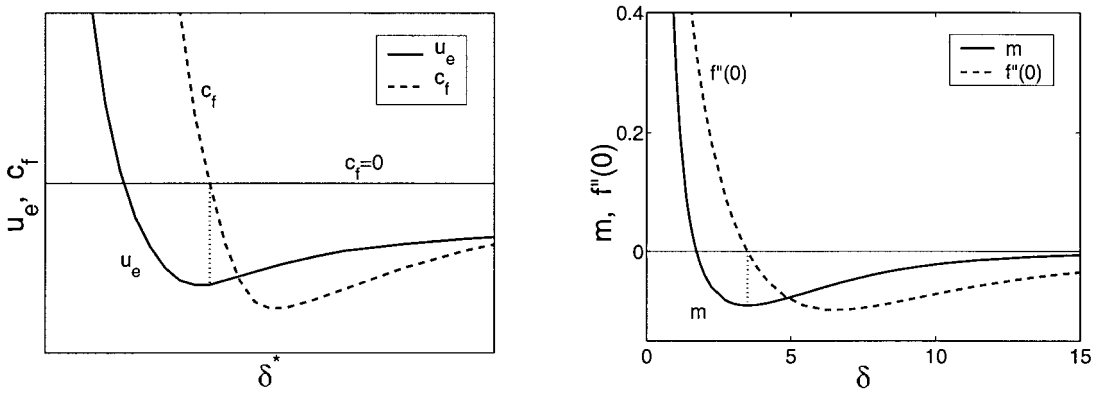

e

Figure 5. Behaviour of u_e and c_f as a function of δ^* at a fixed boundary-layer station (left), and Falkner–Skan relation between pressure parameter m, shear stress $f''(0)$ and displacement parameter δ (right). The left-hand graph is from boundary-layer calculations in 1977; the right-hand graph could have been drawn in 1954.

to correspond (within one or two grid cells) with the point where c_f vanishes, *i.e.* a point of flow separation; Figure 5 (left) gives the idea[2] very resemblant of Figure 4.

All similar studies [34, 35] suggested that the velocity distribution u_e cannot be prescribed arbitrarily near a point of flow separation. There is a certain range in u_e-values outside which no solution seems to exist, a situation correctly predicted by Goldstein some thirty years earlier. In terms of dynamical systems, passing the separation point with u_e prescribed amounts to crossing a saddle point, as explained by Kumar and Yajnik [36]. It would be interesting to study this issue from a theoretical point of view. Only little theory on existence and uniqueness of solutions of the boundary-layer equations exists [37, 38], but with the current numerical evidence it is known what to look for.

In retrospect, it is not difficult to recognize that already earlier similar types of graphs could have been presented, *e.g.* in relation with the family of Falkner–Skan similarity solutions of the boundary-layer equations [39]. This family is governed by the equation

$$f''' + ff'' + \frac{2m}{m+1}(1 - f'^2) = 0, \quad f(0) = f'(0) = 0, \quad f'(\infty) = 1,$$

where m is a parameter related to the pressure gradient through $m = x(\mathrm{d}u_e/\mathrm{d}x)/u_e$. In particular, the main branch of attached flow solutions only exists for $m > -0{\cdot}0904$, whereas for $-0{\cdot}0904 < m < 0$ also a separated flow branch exists; this branch was identified by Stewartson in 1954 [40]. Figure 5 (right) gives an unusual presentation of the Falkner–Skan results: the pressure parameter m and the shear variable $f''(0)$ are shown as a function of the displacement thickness δ (defined through $f(\eta) \sim \eta - \delta$ for $\eta \to \infty$); the resemblance with the much more recent graph in Figure 5 (left) is striking!

[2]The curves have been copied from my research notes of 15 December 1977, drawn in pencil on millimeter paper. The scaling of the axes was not indicated, but it is not relevant: the locations of the minimum in u_e and of the zero of c_f are all that matter.

5. Viscous-inviscid interaction methods

The above, mainly theoretical, considerations brought the insight to tackle engineering boundary-layer problems in an industrial context. The message is twofold: firstly, the boundary-layer approximation is sufficiently accurate to model the flow in mildly separated flow regions; secondly, and most importantly, the hierarchy between boundary layer and inviscid flow is lost. Although for turbulent flow a different asymptotic structure exists [41], the two messages from laminar-flow theory carry over, and in the discussion of Goldstein's singularity the distinction between laminar flow and turbulent flow is irrelevant.

Thus, interactive boundary-layer models were proposed, where Prandtl's boundary-layer equations were coupled with a relation like (10), describing the main interaction with the inviscid flow, or with an accurate inviscid-flow solver. Such a coupled problem can be written as, in principle, two equations with two unknowns:

$$\text{external inviscid flow:} \quad u_e = E[\delta^*], \tag{13}$$

$$\text{boundary-layer flow:} \quad u_e = B[\delta^*]. \tag{14}$$

Here E denotes the external inviscid-flow operator, whereas B is the boundary layer operator for prescribed displacement thickness; note that near flow separation the inverse B^{-1} does not exist.

In the classical, or 'direct', method u_e is computed from the inviscid-flow equation (13), whereas the displacement thickness is determined from the viscous flow (14), with a breakdown of B^{-1} in separation.

Inspired by the theoretical developments described above, in the second half of the seventies a number of ideas have been put forward to circumvent the breakdown singularity. The simplest way is to invert the direction of the iterative process in the classical method. One obtains the so-called 'inverse' method, where, following the idea proposed by Catherall and Mangler [6], the boundary layer is solved with prescribed displacement thickness. An early success was obtained by Carter [42] when he computed the separated flow past an indented plate, by now often used as a benchmark problem [43]. For engineering applications, however, the inverse method converges very slowly and it has not been used on a large scale. To speed up convergence, other methods were developed, of which two have survived [32]: the semi-inverse method of LeBalleur [29, 44] and Carter [45], and the quasi-simultaneous method [46, 47].

5.1. SEMI-INVERSE

The semi-inverse method (Figure 6, left) introduced by LeBalleur in France [29, 44], and independently by Carter in the USA [45], is a mixture of the direct and the inverse method: it solves the boundary-layer equations with prescribed displacement thickness, and the inviscid flow in the traditional way (hence also with prescribed displacement thickness):

$$\begin{aligned} u_e^E = E[\delta^{*(n-1)}] \ \text{(direct)}; \quad u_e^B = B[\delta^{*(n-1)}] \ \text{(inverse)}; \\ \delta^{*(n)} = \delta^{*(n-1)} + \omega \left(u_e^B - u_e^E \right). \end{aligned} \tag{15}$$

In order to obtain convergence, some tuning of the relaxation parameter ω is required, and a fair convergence can be obtained.

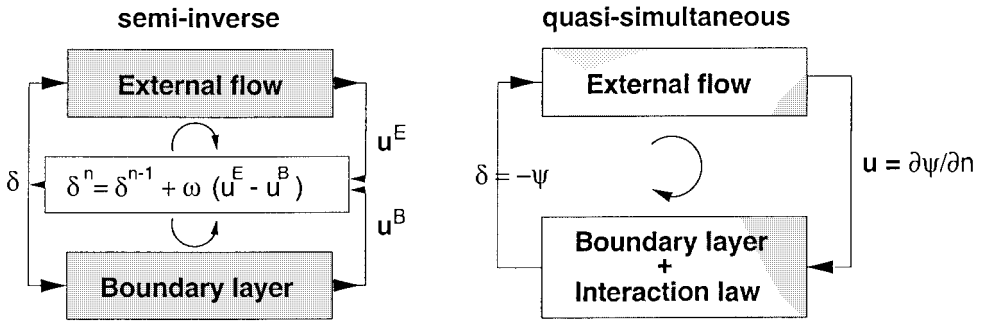

Figure 6. Semi-inverse and quasi-simultaneous VII method.

5.2. QUASI-SIMULTANEOUS

The quasi-simultaneous method follows the suggestion made by Lagerstrom [22]. It wants to reflect the lack of hierarchy between both subdomains: in principle, it wants to solve both subdomain problems simultaneously. When the boundary layer is modelled by an integral formulation a simultaneous coupling is well feasible, *e.g.* [31, 48]; in principle, such an approach has my preference. However, when in both domains a field formulation is chosen, software complexity may prohibit a practical implementation. Recall that around 1980 mainframe computers possessed a memory of only 1(!) Mbyte. At that time this prevented a fully simultaneous approach, and the idea was born to solve the boundary-layer equations simultaneously with a *simple* but good *approximation* of the inviscid flow, which was termed the interaction law. The difference between this approximation and the 'exact' inviscid flow can then be handled iteratively. In this way, the quasi-simultaneous method (Figure 6, right) can be formulated as

$$\begin{aligned} u_e^{(n)} - I[\delta^{*(n)}] &= E[\delta^{*(n-1)}] - I[\delta^{*(n-1)}], \\ u_e^{(n)} - B[\delta^{*(n)}] &= 0, \end{aligned} \tag{16}$$

where the interaction law reads (compare (10))

$$I[\delta^*] = \frac{1}{\pi} \int_\Gamma \frac{d\delta^*}{d\xi} \frac{\mathrm{d}\xi}{x - \xi} \tag{17}$$

(x is still the streamwise boundary-layer coordinate). It is observed in (16) that the interaction law is used in defect formulation, *i.e.* it does not influence the final converged result, but it only enhances the rate of convergence!

Later, when larger computers became available, in engineering applications this simple interaction law has been replaced by more sophisticated ones, for instance interaction laws based on a discrete Laplace description of the inviscid flow (the VILMA method of Arnold and Thiele [49]), or based on an inviscid panel method (*e.g.* Coenen [50]). In this way a better convergence of the iterations in (16) can be obtained. On the other hand, from a scientific point of view, it is interesting to find out how far the above interaction law can be simplified even further. In other words, how close to the traditional 'u_e = prescribed' can the boundary condition for the viscous flow equations be chosen, without being struck by Goldstein's singularity, while at the same time yielding acceptable convergence ot the iterations in (16)?

In three dimensions a similar approach is feasible, with two thin-airfoil expressions like (17) relating the two inviscid surface-velocity components to the shape of the displacement

body, as demonstrated, *e.g.*, by Roget *et al.* [51] and Edwards [52]. The latter author was largely inspired by Davis, who at the east coast of the USA has initiated research in interactive boundary layers [53]. Related work in the UK has been carried out by Smith and co-workers [54]. At the USA west coast Cebeci has been an active advocate of quasi-simultaneous VII methods in engineering applications (airfoil analysis and design) [55]. For three-dimensional engineering flow simulations much pioneering work has been done by Cousteix and his colleagues in France [56].

6. Inclusion of streamline curvature

Especially for rear-loaded airfoils the streamlines immediately behind the trailing edge are highly curved. In such a situation the assumption of constant pressure across the boundary layer is no longer justifiable *a priori.* In asymptotic terms it means that higher-order effects, in regions possibly even smaller than the triple-deck, are becoming relevant.

The effect of streamline curvature can be modelled by a jump between the pressure in the boundary layer p_e and the pressure of the inviscid flow $E_p[\delta^*]$ [32]:

$$p_e = E_p[\delta^*] - [p] \quad \text{with} \quad [p] = \kappa \rho_e u_e^2 (\delta^* + \theta), \tag{18}$$

where κ represents the streamline curvature. The extended version of (16) thus *could* become

$$\begin{aligned} p_e^{(n)} - I_p[\delta^{*(n)}] &= E_p[\delta^{*(n-1)}] - [p]^{(n-1)} - I_p[\delta^{*(n-1)}], \\ p_e^{(n)} - B_p[\delta^{*(n)}] &= 0. \end{aligned} \tag{19}$$

The change of notation from E to E_p will be clear; the influence of streamline curvature is more easy explained in terms of p_e than in terms of u_e.

The pressure jump (18) is proportional to κ, which can be taken as the curvature of the displacement body [32]. Thus, the pressure jump scales with the 'second derivative' of the streamlines and herewith it introduces a strong-interaction character, as will be explained next.

6.1. Asymptotic view

In asymptotic terms the strong-interaction character can be understood as follows. For a plate under angle of attack, *e.g.*, the inviscid trailing-edge streamline, and hence the displacement body, leaves the edge as $y \propto x^{3/2}$, $x \downarrow 0$; therefore its curvature behaves $\propto x^{-1/2}$. The pressure jump (18) then becomes $O(\mathrm{Re}^{-1/2} x^{-1/2})$, and in the inviscid flow a vertical velocity component of the same magnitude is created. In turn, by integrating this vertical velocity in the x-direction, we will create a disturbance $y = O(\mathrm{Re}^{-1/2} x^{1/2})$ in the inviscid position of the trailing-edge streamline. When $x = O(\mathrm{Re}^0)$, for $\mathrm{Re} \to \infty$ this term is smaller than our original starting point $y \propto x^{3/2}$; however when x is smaller than $O(\mathrm{Re}^{-1})$ the disturbance is larger than the original. As in the above triple-deck derivation, a change of hierarchy occurs, indicating strong interaction and requiring a simultaneous treatment.

6.2. Numerical analysis

This reasoning again has a parallel in numerical terms. When the pressure jump is evaluated from a previous iteration as indicated by (19), through κ, in the discretisation of the second derivative of the displacement body it generates a contribution to the iterative amplification

factor proportional to $(\delta x)^{-2}$, where δx is the mesh size. If we allow the mesh size to approach zero, this amplification blows up, as in the above asymptotic view when x tends to zero. This explains the numerical difficulties encountered in the literature when the curvature effect is not treated in a simultaneous way [32, p. 82]. Extensive smoothing and underrelaxation is then required to obtain convergence of the viscous-inviscid iterations, as stated by [57] and references therein.

Once again a simultaneous treatment of the curvature effect is required. The term $[p]^{(n-1)}$ should be shifted to the left-hand side in (19) and evaluated at the new iteration level (n). However, this necessary step to obtain convergence for small grid size turns out not to be sufficient. There is another (delicate) issue, which can be understood through a generalization of the analysis in [58]. Let us assume that the curvature is computed from the displacement body, *i.e.* $\kappa = \mathrm{d}^2\delta^*/\mathrm{d}x^2$. Then the pressure jump (18) becomes

$$[p] = \rho_e u_e^2(\delta^* + \theta)\frac{\mathrm{d}^2\delta^*}{\mathrm{d}x^2} \quad \text{to be abbreviated as} \quad [p] = c\frac{\mathrm{d}^2\delta^*}{\mathrm{d}x^2}.$$

The quasi-simultaneous system (19) now reads

$$\begin{aligned} p_e^{(n)} - I_p[\delta^{*(n)}] + c\frac{\mathrm{d}^2}{\mathrm{d}x^2}\delta^{*(n)} &= E_p[\delta^{*(n-1)}] - I_p[\delta^{*(n-1)}], \\ p_e^{(n)} - B_p[\delta^{*(n)}] &= 0. \end{aligned} \tag{20}$$

Since both I_p and $\mathrm{d}^2/\mathrm{d}x^2$ are negative-(semi)definite operators, and since $c > 0$, the two operators mentioned counteract each other in the left-hand side of (20)! Moreover, since the discrete version of I_p scales with $(\delta x)^{-1}$, whereas the curvature term scales with $(\delta x)^{-2}$, the unfavourable influence of the latter can be made arbitrarily large for vanishing grid size. The envisaged iterations will not converge, and there is only one way out of this problem: discretize the second derivative with a one-sided expression

$$\left.\frac{\mathrm{d}^2\delta^*}{\mathrm{d}x^2}\right|_i = \frac{\delta^*_{i-2} - 2\delta^*_{i-1} + \delta^*_i}{(\delta x)^2} \tag{21}$$

(the downstream-biased version will also work). At least in this way the eigenvalues of the discrete operator in (21) are positive, and hence of the same sign as those of $-I_p$. Numerical experiments with the usual central discretization of the second derivative and with the above upstream-biased one have consistently revealed that only the latter one could be made convergent (at least for not too violent flow cases, which probably is related to the onset of wake instability – more research is required here). An in-depth theoretical discussion of this issue will be presented in a forthcoming publication [59].

7. Application to transonic airfoil flow

The performance of the quasi-simultaneous coupling concept will be demonstrated on a typical calculation of transonic flow past an RAE 2822 airfoil with the NLR Vistrafs code. The boundary layer was modelled by Prandtl's equations with the algebraic Cebeci-Smith turbulence model; effects of streamline curvature were included. The inviscid flow was modelled by transonic full potential theory. As an interaction law, the integral (17) has been used to describe the symmetric displacement effects ('thickness problem'), together with its skew-symmetric

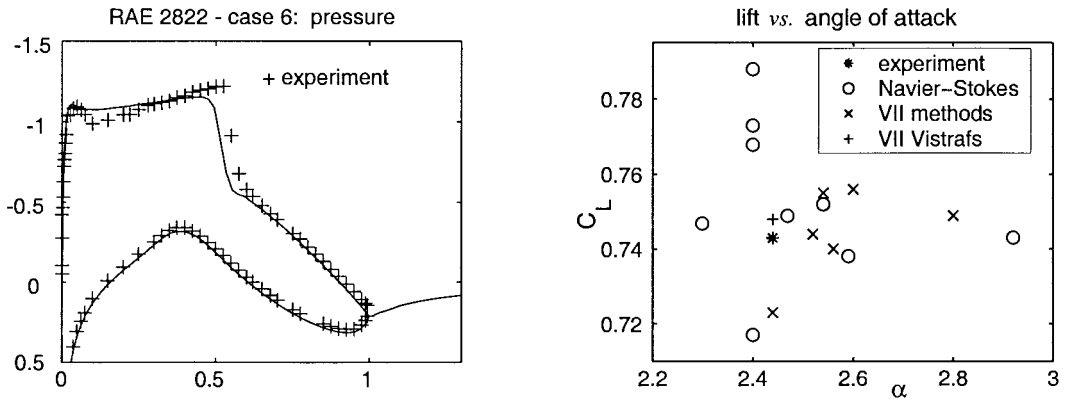

Figure 7. RAE 2822 airfoil at M=0·725, Re=6·5mill., α=2·44, C_L=0·743 (Case 6). Pressure distribution (left) and comparison of lift predictions by various VII and NS methods [61] (right).

counterpart to describe the effects of camber ('lift problem'); for details see Veldman et al. [59, 60].

The flow case presented in Figure 7 is mildly transonic, with a small amount of separated flow near the trailing edge. Pertinent flow parameters are $M = 0{\cdot}725$, Re $= 6{\cdot}5$ million, $\alpha_{\text{exp}} = 2{\cdot}92$ (with a corrected value of $\alpha = 2{\cdot}44$) and fixed transition at 3% chord.

The computational grid consists of 173×21 gridpoints (C-type, with 128 points along the airfoil surface) in the boundary layer, and the inviscid-flow grid was 128×64 (O-type). The computations require about 10 quasi-simultaneous iterations to converge to 3–4 digits, which on a modern PC takes less than one minute (it was so much different in the mid-eighties when this method was developed ...). The rate of convergence is governed by the difference between the exact inviscid flow E and its approximation I; as a consequence it is independent of grid size. To appreciate the fast convergence even better, one has to realize that the external flow in this example is transonic, with a significant supersonic flow region, whereas the interaction law (17) is based on sub(!)sonic theory.

In 1986 this flow case has been the subject of a workshop [61], where about twenty aerodynamic codes were compared. The lift coefficient predicted by these codes is presented in Figure 7 (right), where a distinction has been made between viscous-inviscid interaction (VII) codes and Navier–Stokes codes. A similar situation was found for the other flow cases investigated in the workshop. The participants were also requested to quantify the computational complexity of their codes: it was found that, depending on the inviscid flow model used, VII codes were one to two orders of magnitude cheaper than Navier–Stokes codes. The latter codes required 10^6–10^7 floating-point operations per grid point; a price tag that is still representative for today's Navier–Stokes codes, as can be inferred from the review data presented by Agarwal [62].

A conclusion of the workshop must be that, in spite of their much smaller complexity, the quality of the VII results is comparable to that of the Navier–Stokes results. In fact, the quality of flow simulations for this type of flow appears to be dominated by the quality of the turbulence model. Any difference between a full Navier–Stokes model and a simplified boundary-layer model just drowns in the uncertainty inherent in turbulence modelling. As stated by Holst [61]: "An engineering turbulence model that can approximately predict the size and extent of separated regions is desperately needed." Since 1986 the situation has not changed significantly. A European CFD validation project in 1992 once again revealed that

the uncertainty due to turbulence modelling produces a large spreading of the Navier–Stokes results [63].

Of course, Navier–Stokes modelling is required in situations where the viscous region can no longer be regarded as thin, such as massive flow separation in take-off and landing configurations, or the flow near essentially three-dimensional objects. In this respect it is remarkable that maximum-lift prediction with a VII method appears to be feasible, as demonstrated by Cebeci and co-workers [55, 64].

8. Concluding remarks

Prandtl's 1904 boundary-layer theory formed the starting point for the viscous-inviscid interaction methods that have been developed in the last two decades of the 20th century. They have become very popular, since in comparison with brute-force Navier–Stokes solutions they are about two orders less expensive, whereas for flow conditions with thin shear layers the results are equally useful. Because of their modest computational complexity, they are ideal for use in aerodynamic-airfoil and wing-optimization studies, *e.g.* [65, 66, 67, 68].

The greatest challenge has been to understand and resolve the singularity at separation, which occurs when the boundary-layer equations are solved with prescribed pressure. In 1948, Goldstein already foresaw the possibility that near separation in general no solution does exist, unless the pressure satisfies certain properties. Triple-deck theory provided the insight behind these difficulties, and gave the clue towards their solution. Goldstein turns out to have pointed in the right direction of non-existence; doubts on the validity of the boundary-layer model were found not to be essential here.

Stewartson and his 1969 contemporates have provided the asymptotic framework valid near separation: the triple deck. In 1975 Lagerstrom described his view on the triple deck, and today we know that his paper contains the essential message required to overcome the singularity at a point of flow separation: boundary-layer and inviscid flow have to be solved simultaneously. It is through this type of insight that the use of viscous-inviscid interaction methods in engineering applications can flourish.

Only a small, strongly personally biased, glimpse of the world-wide struggle between Prandtl's boundary-layer concept and the numerical simulation of separated flow could be shown in the paper: we have emphasised steady incompressible flow, and scratched only superficially supersonic inviscid flow and unsteady flow separation. Many instances can be found in the literature which, in retrospect, were close to unraveling the correct view, but lack of computational power preventing further pursuit. It would be interesting to analyse all these 'close encounters', and I hope to find another occasion to dig deeper into this intrigueing 20th-century story.

References

1. L. Prandtl, Ueber Fluessigkeitsbewegung mit kleiner Reibung. In: *Verhandlungen des dritten internationalen Mathematischen Kongresses*. Heidelberg. Leipzig: Teubner Verlag (1905) pp. 484–491.
2. K. Stewartson, D'Alembert's paradox. *SIAM Review* 23 (1981) 308–343.
3. M. Van Dyke, Nineteenth-century roots of the boundary-layer idea. *SIAM Review* 36 (1994) 415–424.
4. M.J. Lighthill, On displacement thickness. *J. Fluid Mech.* 4 (1958) 383–392.
5. S. Goldstein, On laminar boundary layer flow near a point of separation. *Quart. J. Mech. Appl. Math.* 1 (1948) 43–69.

6. D. Catherall and K.W. Mangler, The integration of the two-dimensional laminar boundary-layer equations past the point of vanishing skin friction. *J. Fluid Mech.* 26 (1966) 163–182.
7. M.J. Lighthill, On boundary layers and upstream influence I. A comparison between subsonic and supersonic flows. *Proc. R. Soc. London* A 217 (1953) 478–507.
8. K. Stewartson, On the flow near the trailing edge of a flat plate II. *Mathematika* 16 (1969) 106–121.
9. K. Stewartson and P.G. Williams, Self-induced separation. *Proc. R. Soc. London* A 312 (1969) 181–206.
10. A.F. Messiter, Boundary-layer flow near the trailing edge of a flat plate. *SIAM J. Appl. Math.* 18 (1970) 241–257.
11. V.Ya. Neiland, Towards a theory of separation of the laminar boundary layer in a supersonic stream. *Mekh. Zhid. Gaza*, 4 (1969) 53–57 (English translation in *Fluid Dynamics* 4 (1970) 33-55).
12. R.E. Meyer, A view of the triple deck. *SIAM J. Appl. Math.* 43 (1983) 639–663.
13. K. Stewartson, Multi-structured boundary layers on flat plates and related bodies. *Adv. in Applied Mech.* 14 (1974) 145–239.
14. F.T. Smith, On the high-Reynolds number theory of laminar flows. *IMA J. Appl. Math.* 28 (1982) 207–281.
15. F.T. Smith, Steady and unsteady boundary-layer separation. *Ann. Rev. Fluid Mech.* 18 (1986) 197-220.
16. F.T. Smith and J.H. Merkin, Triple-deck solutions for subsonic flow past humps, steps, concave or convex corners and wedged trailing edges. *Comp. Fluids* 10 (1992) 7–25.
17. A.P. Rothmayer and F.T. Smith, Numerical solution of two-dimensional steady triple-deck problems. In: R.W. Johnson (ed.) *The Handbook of Fluid Dynamics*. Boca Raton: CRC Press (1998) Chapter 25.
18. V.V. Sychev, A.I. Ruban, V.V. Sychev and G.L. Korolev, *Asymptotic Theory of Separated Flows.* Cambridge: Cambridge University Press (1998) 352 pp.
19. C.E. Jobe and O.R. Burggraf, The numerical solution of the asymptotic equations of trailing edge flow. *Proc. R. Soc. London* A 340 (1974) 91–111.
20. R.E. Melnik and R. Chow, *Asymptotic Theory of Two-dimensional Trailing Edge Flows*. Grumman Research Department, Report RJ-510J (1975).
21. A.E.P. Veldman and A.I. van de Vooren, Drag of a finite flat plate. In: R.D. Richtmayer (ed.) Proc. 4th Int. Conf. Num. Meth. Fluid Dyn., *Lecture Notes in Physics* 35. Berlin: Springer Verlag (1976) pp. 422–430.
22. P.A. Lagerstrom, Solutions of the Navier–Stokes equation at large Reynolds number. *SIAM J. Appl. Math.* 28 (1975) 202–214.
23. W.D. Hayes and R.F. Probstein, *Hypersonic Flow Theory.* Academic Press (1959) 464 pp.
24. K. Stewartson, F.T. Smith and K. Kaups, Marginal separation. *Stud. Appl. Math.* 67 (1982) 45–61.
25. J.W. Elliott and F.T. Smith, Dynamic stall due to unsteady marginal separation. *J. Fluid Mech.* 179 (1987) 489–512.
26. L.L. van Dommelen and S.F. Shen, The spontaneous generation of the singularity in a separating laminar boundary layer. *J. Comput. Phys.* 38 (1980) 125–140.
27. R.A.W.M. Henkes and A.E.P. Veldman, On the breakdown of the steady and unsteady interacting boundary-layer description. *J. Fluid Mech.* 179 (1987) 513-529.
28. H. Schlichting and K. Gersten, *Boundary-Layer Theory*, 8th revised and enlarged edition. Berlin: Springer (2000) 799 pp.
29. J.C. LeBalleur, Couplage visqueux-non visqueux: analyse du problème incluant décollements et ondes de choc. *La Recherche Aérospatiale* 1977-6 (1977) 349–358.
30. R.C. Lock, Prediction of the drag of wings at subsonic speeds by viscous-inviscid interaction techniques. In: AGARD-R-723 (1985) paper 10.
31. R. Houwink and A.E.P. Veldman, Steady and unsteady separated flow computation for transonic airfoils. AIAA paper 84–1618 (1984).
32. R.C. Lock and B.R. Williams, Viscous-inviscid interactions in external aerodynamics. *Prog. Aerospace Science* 24 (1987) 51–171.
33. A.E.P. Veldman, Boundary layers with strong interaction: from asymptotic theory to calculation method. In: J.J.H. Miller (ed.), *Proc. BAIL 1 Conf. on Boundary and Interior layers*. Dublin: Boole Press (1980) pp. 149–163.
34. P. Ardonceau, Th. Alziary and D. Aymer, Calcul de l'interaction onde de choc/couche limite aves décollement. In: *Computation of Viscous-Inviscid Interactions*, AGARD-CP-291 (1980) paper 28.
35. H.P. Horton, Numerical investigation of regular laminar boundary layer separation. In: *Flow Separation*, AGARD-CP-168 (1975) paper 7.

36. A. Kumar and K.S. Yajnik, Internal separated flows at large Reynolds number. *J. Fluid Mech.* 97 (1980) 27–51.
37. K. Nickel, Prandtl's boundary-layer theory from the viewpoint of a mathematician. *Ann. Rev. Fluid Mech.* 5 (1973) 405–428.
38. W. Walter, Existence and convergence theorems for the boundary layer equations based on the line method. *Arch. Rat. Mech. Anal*. 39 (1970) 169–188.
39. V.M. Falkner and S.W. Skan, Solutions of the boundary layer equation. *Phil. Mag.* 12 (1931) 865–896.
40. K. Stewartson, Further solutions of the Falkner-Skan equation. *Proc. Cambridge Phil. Soc.* 50 (1954) 454-465.
41. R.E. Melnik, R. Chow and H.R. Mead, Theory of viscous transonic flow over airfoils at high Reynolds number. AIAA paper 77-680 (1977).
42. J.E. Carter and S.F. Wornom, Solutions for incompressible separatedd boundary layers including viscous-inviscid interaction. In: *Aerodynamic Analysis Requiring Advanced Computers.* NASA SP-347 (1975) pp. 125–150.
43. T. Cebeci, H.H. Chen and J.A. Majeski, Indented plate problem revisited. *Int. J. Num. Meth. Fluids* 16 (1993) 391–401.
44. J.C. LeBalleur, Couplage visqueux-non visqueux: méthode numérique et applications aux écoulements bidimensionnels transsoniques et supersoniques. *La Recherche Aérospatiale* 183 (1978) 65–76.
45. J.E. Carter, Viscous-inviscid interaction analysis of turbulent separated flow. AIAA paper 81–1241 (1981).
46. A.E.P. Veldman, A numerical method for the calculation of laminar incompressible bounday layers with strong viscous-inviscid interaction. National Aerospace Laboratory, Report NLR TR 79023 (1979).
47. A.E.P. Veldman, New, quasi-simultaneous method to calculate interacting boundary layers. *AIAA J.* 19 (1981) 79–85.
48. M. Drela and M.B. Giles, Viscous-inviscid analysis of transonic and low Reynolds number airfoils. *AIAA J.* 25 (1987) 1347–1355.
49. F. Arnold and F. Thiele, Laplace interaction law for the computation of viscous airfoil flow in low- and high-speed aerodynamics. *AIAA J.* 31 (1994) 2178–2185.
50. E.G.M. Coenen, Quasi-simultaneous coupling for wing and airfoil flow. In: C.-H. Lai, P.E. Bjorstad, M. Cross and O.B. Widlund (eds.), *Domain Decomposition Methods in Science and Engineering*. Bergen: Domain Decomposition Press (1999) pp. 197–205.
51. C. Roget, J.Ph. Brazier, J. Cousteix and J. Mauss, A contribution to the physical analysis of separated flows past three-dimensional humps. *Eur. J. Mech. B* 17 (1998) 307–329.
52. D.E. Edwards, Analysis of three-dimensional separated flow using interacting boundary-layer theory. In: F.T. Smith and S.N. Brown (eds.), *Boundary-Layer Separation.* Berlin: Springer Verlag (1987) pp. 163–178.
53. M.J. Werle, R. Thomas Davis — His contributions to numerical simulation of viscous flows: Part II — Technical perspective. AIAA paper 88–0602 (1988).
54. F.T. Smith, Steady and unsteady 3-d interactive boundary layers. *Comp. Fluids* 20 (1991) 243–268.
55. K.C. Chang, N. Alemdaroglu, U, Mehta and T. Cebeci, Further comparisons of interactive boundary-layer and thin-layer Navier-Stokes procedures. *J. Aircraft* 25 (1988) 897–903.
56. J. Cousteix, Three-dimensional and unsteady boundary-layer computations. *Ann. Rev. Fluid Mech.* 18 (1986) 173–196.
57. G. Dargel and P. Thiede, Viscous transonic airfoil flow simulation by an efficient viscous-inviscid interaction method. AIAA paper 87–0412 (1987).
58. A.E.P. Veldman, A numerical view on strong viscous-inviscid interaction. In: W.G. Habashi (ed.), *Computational Methods in Viscous Flows*. Southampton: Pineridge Press (1984) pp. 343–363.
59. A.E.P. Veldman and M.A.M. Somers, The inclusion of streamline curvature in a quasi-simultaneous viscous-inviscid interaction method for transonic airfoil flow. Preprint available at `http://www.math.rug.nl/~veldman/preprints.html` (1999).
60. A.E.P. Veldman, J.P.F. Lindhout, E. de Boer and M.A.M. Somers, VISTRAFS: a simulation method for strongly-interacting viscous transonic flow. In: T. Cebeci (ed.), *Numerical and Physical Aspects of Aerodynamic Flow IV*. Berlin: Springer Verlag (1990) pp. 37–51.
61. T.L. Holst, Viscous Transonic Airfoil Workshop - Compendium of Results. AIAA paper 87–1460 (1987).
62. R. Agarwal, Computational fluid dynamics of whole-body aircraft. *Ann. Rev. Fluid Mech.* 31 (1999) 125–169.

63. W. Haase, F. Brandsma, E. Elsholz, M. Leschziner and D. Schwamborn (eds.), *EUROVAL — An European Initiative on Validation of CFD Codes*. Notes on Numerical Fluid Mechanics 42. Braunschweig: Vieweg (1993) 530 pp.
64. T. Cebeci, H. Hefazi, F. Roknaldin and L.W. Carr, Predicting stall and post-stall behaviour of airfoils at low Mach numbers. *AIAA J.* 33 (1995) 595–602.
65. A.J. van der Wees and J. van Muijden, A fast and robust viscous-inviscid interaction solver for transonic flow about wing/body configurations on the basis of full potential theory. AIAA paper 93–3026 (1993).
66. P.D. Smith, A viscous package for attached and separated flows on swept and tapered wings. RAE Technical Report 89027 (1989).
67. M. Drela and M.B. Giles, ISES: a two-dimensional viscous aerodynamic design and analysis code. AIAA paper 87–1118 (1987).
68. A. Verhoff, H.H. Chen, T. Cebeci and T. Michal, An accurate and efficient interactive boundary-layer method for analysis and design of airfoils. AIAA paper 96–0328 (1996).